Weighted-residual integral boundary-layer model for nonlinear dynamics of falling liquid films

Alexander Oron, O. Gottlieb and Elena Novbari

Department of Mechanical Engineering, Technion-Israel Institute of Technology, Haifa 32000, ISRAEL

E-mail: meroron@tx.technion.ac.il

Abstract. The nonlinear dynamics of thin liquid films falling on a vertical plane is investigated numerically using the first-order time-dependent weighted-residual integral boundary layer (WRIBL) equations derived by Ruyer-Quil and Manneville (2000). We find that sufficiently close to the stability threshold of the system with periodic boundary conditions, the emerging waves are of γ_1-type. However, beyond a secondary bifurcation threshold, γ_2-type waves emerge and can coexist with γ_1 waves. The analysis of the WRIBL equations reveals the existence of both periodic traveling wave (TW) and aperiodic non-stationary wave (NSW) flows. The bifurcation structure of WRIBL equations is found to include three distinct regions: (i) linearly stable, (ii) bounded wave flows, (iii) reverse-flow solutions.

1. Introduction

Falling liquid films are often encountered in various technological applications, such as evaporators, condensers, heat exchangers, coating, and physical phenomena, such as gravity currents and lava flows. Significant progress has been attained in the analysis of thin (macroscopic) liquid films. Oron *et al.* [1] unified such analyses into a comprehensive framework in which the special cases naturally emerged. Employing the long-wave approximation Oron *et al.* [1] derived a generic evolution equation describing the spatio-temporal dynamics of a liquid film subjected to various physical mechanisms.

Along with direct numerical simulations of the dynamics of falling film flows, several model evolution equations were derived using various asymptotic approaches in the longwave limit. Among these one finds Benney [2] and Shkadov equations [3]. A novel analytical approach was introduced by Ruyer-Quil and Manneville [4, 5] extending the boundary-layer theory developed by Shkadov [3]. The Shkadov theory was shown [6, 7] to be successful in describing the dynamics of falling films on static vertical and inclined substrates for intermediate Reynolds numbers ($R < 300$). However, it failed to match the linear stability threshold of the system, as was derived by Benjamin [8] using Orr-Sommerfeld equations and by Yih [9] employing long-wave expansions. The theory developed by Ruyer-Quil and Manneville [4, 5] for both first- and second-order approximations of the Navier-Stokes equations can be classified as weighted-residual integral boundary layer (WRIBL) theory. It corrected the inability of the Shkadov model equations to match the linear stability threshold of the system and was found to yield bounded solutions for a wide range of Reynolds numbers. Recently, Scheid et al. [10] carried out the investigation of traveling wave solutions of the first-order WRIBL equations with various boundary conditions.

However, the time-dependent evolution of the falling films, as described by the first-order WRIBL equations with periodic boundary conditions, has not yet been investigated.

The objective of this paper is to investigate the nonlinear dynamics of falling films on a vertical plane in the framework of the first-order *time-dependent* WRIBL equations augmented by periodic boundary conditions and to compare with the results of the studies of the WRIBL equations derived for traveling wave solutions [10].

2. Governing evolution equations

We consider a two-dimensional flow of an isothermal liquid film of the average thickness d on a solid vertical planar surface in the gravity field g. The relevant properties of the liquid are density ρ, kinematic viscosity ν and surface tension σ.

In order to analyze the spatio-temporal evolution of the film interface we employ here the first-order WRIBL evolution equations derived by Ruyer-Quil and Manneville [4] in the non-dimensional form

$$h_t + q_x = 0, \tag{1}$$

$$q_t = \frac{5}{6}h + \frac{5}{6}\kappa h h_{xxx} - \frac{5}{2}\,\frac{q}{h^2} - \frac{17}{7}\,\frac{qq_x}{h} + \frac{9}{7}\,\frac{q^2 h_x}{h^2}. \tag{2}$$

Here $h = h(x,t), q = q(x,t)$ are, respectively, the local film thickness and the leading-order approximation of the volumetric flow rate

$$q = \int_0^h u\ dy. \tag{3}$$

Both h and q depend on the spatial coordinate along the solid plane x and time t, u is the leading-order longitudinal, x-component of the non-dimensional flow field, y is the spatial direction normal to the wall, and κ is the Kapitza number given by

$$\kappa = \frac{\sigma}{\rho\nu^{4/3}g^{1/3}}. \tag{4}$$

Equations (1),(2) are written in dimensionless form, while the dimensionless spatial coordinate x and film thickness h, time t, the longitudinal fluid velocity component u and the flow rate q scale the corresponding physical variables in terms of viscous length $l_\nu = (\nu^2/g)^{1/3}$, viscous time $t_\nu = (\nu/g^2)^{1/3}$, viscous velocity $U_\nu = (\nu g)^{1/3}$ and the value $U_\nu l_\nu$, respectively.

Equations (1),(2) are hereafter numerically solved with periodic boundary conditions for both h and q in the domain $0 \le x \le L$ and for various initial conditions, one of them, namely

$$h(x,t=0) \equiv h_0(x) = h_N + \delta \sin\left(\frac{2\pi x}{L}\right),\ \delta \ll 1,\ q(x,t=0) \equiv q_0(x) = q_N, \tag{5}$$

is referred to as a "standard" initial condition. The value of δ is typically varied between 0.05 and 0.1. Note that the boundary-value problem at hand, Eqs.(1),(2),(5), is governed by two parameters, one of which κ is a pure material property and the other, h_N is related to the strength of the velocity field.

The values h_N and q_N appearing in Eqs.(5) are related to the Reynolds number based on the maximal value of the film velocity

$$R = \frac{gd^3}{2\nu^2} \tag{6}$$

via

$$h_N = (2R)^{1/3},\ q_N = \frac{1}{3}h_N^3, \tag{7}$$

respectively, the film thickness and the volumetric flow rate of the base Nusselt flow.

In order to compare the results of our investigation with other work available in the literature, it is important to relate between various values used elsewhere. Oron and Gottlieb [11] employed in their investigations of the first-order Benney equation the parameters R, the rescaled Weber number $\tilde{S}$ given by

$$\tilde{S} = \frac{2\sigma}{3\rho g d^2} \tag{8}$$

and the small order parameter ε defined as the ratio between the mean film thickness and the characteristic wavelength of the interfacial disturbance. We note that Scheid et al. [10] used the value of the Reynolds number based on the average film velocity, $Re = \frac{2}{3}R$, and the value of the fundamental wavenumber k corresponding to the size of the periodic domain of L. These values are related in addition to the relationships given in Eq.(7) by

$$L = \frac{2\pi}{k},\ \varepsilon = \frac{kh_N}{2\pi},\ \kappa = Wh_N^2. \tag{9}$$

In what follows, we will adopt the notation of R, ε and W employed in [11].

The first observation that can be made on the basis of Eqs.(1),(2) is that if their solution is a traveling wave (TW) moving with the speed c, $h = h(\xi), q = q(\xi)$ with $\xi = x - ct$, then Eq.(1) implies that

$$q(\xi) = ch(\xi) + A, \tag{10}$$

where A is a constant. However, in spite of this simplification Eqs.(1),(2) cannot be further reduced, as the obtained set of equations will in this case consist of the ordinary differential equation arising from Eq.(2) with two unknown constant values c and A. Moreover, as will be demonstrated below, not all solutions of Eqs.(1),(2) are TW.

3. Linear stability analysis of Eqs.(1),(2)

We linearize Eqs.(1),(2) with $B = 0$ around the base state $h = h_N,\ q = q_N$ with $h = h_N + \bar{\delta}\bar{h},\ q = q_N + \bar{\delta}\bar{q},\ \bar{\delta} \ll 1$, and introduce normal mode perturbations in the form of

$$\bar{h} = \eta \exp(ikx + \omega t),\ \bar{q} = \zeta \exp(ikx + \omega t), \tag{11}$$

where $k = 2\pi n/L$ and ω are their wavenumber and complex growth rate, respectively, and n is the integer number of the harmonics. Substituting Eq.(11) into the linearized version of Eqs.(1), (2) yields the dispersion relation

$$\omega^2 + \omega(\frac{5}{2h_N^2} + \frac{17}{7}ik\frac{q_N}{h_N}) + ik[\frac{5}{6} + \frac{5q_N}{h_N^3} + ik(\frac{9q_N^2}{7h_N^2} - \frac{5}{6}k^2\kappa h_N)] = 0. \tag{12}$$

The value of $\omega = 0$ cannot satisfy Eq.(12), therefore the instability can set in only via Hopf bifurcation, as expected by observation of the system at hand. Assuming that one of the eigenvalues ω to be purely imaginary $\omega_1 = i\Omega$ and the other to be a general complex number $\omega_2 = \alpha + i\beta$, leads to the following values of the unknowns

$$\alpha = -\frac{5}{2h_N} < 0,\ \Omega = -kh_N^2 < 0,\ \beta = \frac{4}{21}kh_N^2. \tag{13}$$

The negative sign of α suggests that the second mode, corresponding to ω_2 is stable for all n. The negative sign of Ω suggests that the wave propagates in the downward direction, i.e., in the direction of positive x. The dimensionless wave celerity at the stability threshold of the system (critical frequency) is obtained from Eqs.(12),(13) as

$$c_1 = h_N^2. \tag{14}$$

The stability threshold for the n-th mode is also obtained from Eqs.(12),(13) in the form

$$R = R_n = 5\kappa(\frac{n\pi}{L})^2,\ n = 1, 2, \ldots, \tag{15}$$

and, in particular, the Hopf stability threshold of the system is given by

$$R = R_1 = \frac{5}{4}\kappa(\frac{2\pi}{L})^2. \tag{16}$$

We will hereafter concentrate on two specific cases referred to as case A, in which $W = 1000, \varepsilon = 0.04/2\pi$ (equivalent to $\kappa k^2 = 1.6$), and case B, in which $W = 1000, R = 3.1$ (equivalent to $\kappa = 3374.9, h_N = 1.837$). These two cases facilitate the comparison with the previous studies related to the Benney equation [11, 12] and to Eqs.(1),(2) [10].

It follows, therefore, from Eq.(15) that in case A ($W = const, \varepsilon = const$)

$$R_n = n^2 R_1,\ n = 1, 2, \ldots \tag{17}$$

with $R_1 = 2$ for the chosen values of W and ε. Similarly, it follows from Eq.(15) that in case B ($W = const, R = const$)

$$\varepsilon_n = \frac{\varepsilon_1}{n},\ n = 1, 2, \ldots \tag{18}$$

with

$$\varepsilon_1 = (R_1/5W)^{1/2}/\pi, \tag{19}$$

which yields $\varepsilon_1 \approx 0.007926$ for the chosen values of W and R. as obtained for the Benney equation [11, 12].

Figure 1 displays the stability diagram of the falling film for $W = 1000$. The curve $n = 1$ represents the Hopf stability threshold, as given by Eq.(19), and divides the $\varepsilon - R$ plane into two domains, one of which (I), located above this curve is the domain of linear stability of the system, while the other (II and III combined), below the curve is that of its instability. The curves $n = 2$ to $n = 6$ show the stability thresholds of the respective n-th modes, as given by Eq.(18). Both, horizontal and vertical dot-dashed lines show the ranges, where our numerical investigation has been carried out in cases A and B, respectively. The domain of the film instability, i.e. below the curve $n = 1$, is further subdivided into two subdomains II and III, where the boundary between these is the dashed line marked by black circles.

4. Numerical investigation

It is readily seen that Eqs.(1),(2) are not invariant under the transformation $h \to h_N - h,\ q \to q_N - q$, hence their solutions are not expected to be symmetric with respect to the equilibrium state, $h = h_N,\ q = q_N$. Thus, in general $h_{max} - h_N \neq h_N - h_{min}$. To characterize the asymmetric solutions for Eqs.(1),(2) we use here the classification made by Chang [7] for the waves emerging in falling liquid films: (i) the γ_1-family whose representatives satisfy the condition $h_{max} - h_N < h_N - h_{min}$, i. e., depression or "hole" waves, and (ii) the γ_2-family whose representatives satisfy the condition $h_{max} - h_N > h_N - h_{min}$, i. e. elevation or "hump" waves.

4.1. Case A

4.1.1. Bifurcation structure As noted above, the stability threshold of the system in case A is given by $R = R_1 = 2$. To investigate the film dynamics in the unstable domain we solve Eqs.(1),(2) numerically in the range of $2 < R \leq 35$ ($1.587 < h_N \leq 4.121$) and the results are shown hereafter. Figure 2 presents the normalized amplitude $H = h_{max}/h_N$ of the film thickness given by the solution for Eqs.(1),(2) reached after the transient period as a function of R. In

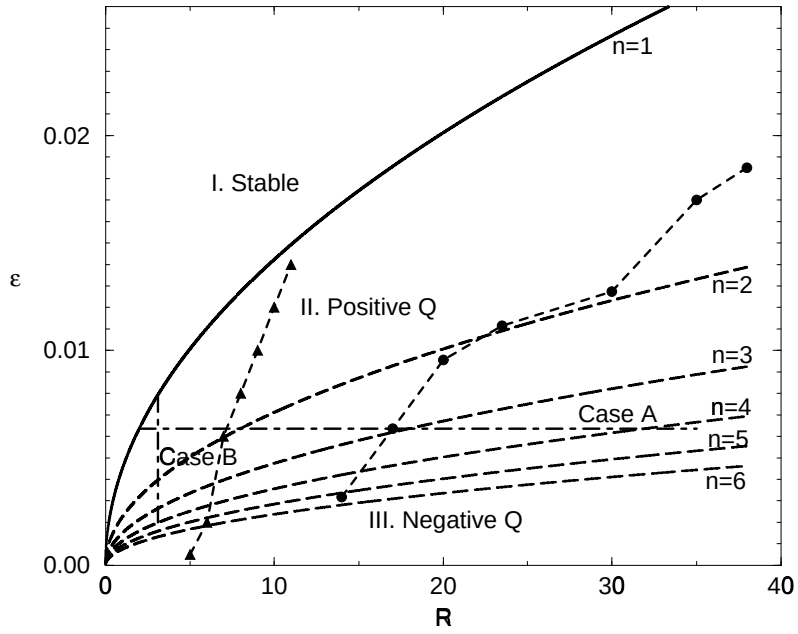

Figure 1. Stability diagram for Eqs.(1),(2) as presented in the $\varepsilon - R$ plane. The curves $n = 1$ to $n = 6$ given by Eqs.(18),(19) show the instability thresholds for the n-th mode, thus $n = 1$ is the instability threshold of the system. The horizontal and vertical dot-dashed lines indicate the parameter values investigated here in the framework of cases A and B, respectively. The dashed curve marked with black circles displays the border line below which the value of Q becomes negative.

this figure the value of H is indicated by an appropriate point when the corresponding solution is a traveling wave (TW), and by a bar showing the variation range of H in the large-time limit when the corresponding solution is a non-stationary wave (NSW). It is found that the solutions in the domain $2 < R < 6.6$ ($1.587 < h_N < 2.363$) are TW of the γ_1-family, represented by the solution for $R = 5$ ($h_N = 2.154$). In the range of $6.7 \leq R \leq 7.6$ ($2.375 \leq h_N \leq 2.477$), we find coexisting TW of both γ_1- and γ_2-families. The abrupt termination of the γ_2-branch at $R \approx 6.7$ ($h_N \approx 2.477$) suggests the existence of secondary subcritical pitchfork bifurcation at $R = \hat{R}$, and due to this, the existence of another, unstable TW branch in the interval $6.6 < R < \hat{R}$. This unstable branch cannot be recovered by numerical solution of the pertinent partial differential equations. In the domains $7.7 \leq R \leq 31$ ($2.488 \leq h_N \leq 3.958$) and $33 \leq R \leq 35$ ($4.041 \leq h_N \leq 4.121$), TW of the γ_2-family are only present. We also find that solutions of Eqs.(1),(2) within the interval $31.5 \leq R \leq 32.5$ ($3.979 \leq h_N \leq 4.021$) are NSW.

4.1.2. Traveling wave solutions The results of our computations show that in the vicinity of $R = R_n$, the number of wave humps increases by one complying with the results of the linear theory. However, we have not found replicated waves defined by TW flows consisting of two or more identical humps, and all multi-humped flows we have obtained, consist of one major wave and one or more smaller ones.

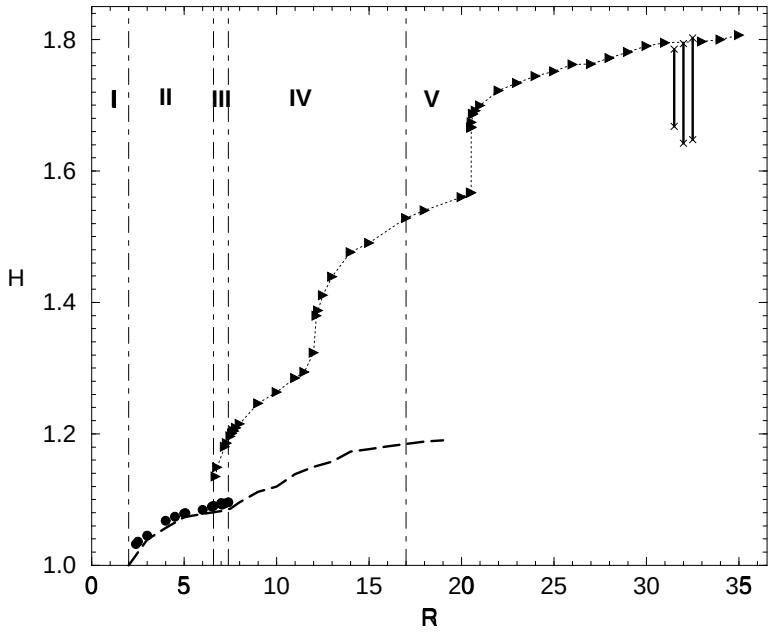

Figure 2. The bifurcation diagram for case A, as obtained from Eqs.(1),(2), that shows the value of the normalized wave amplitude H as a function of R. The black circles and triangles represent TW flows of the γ_1- and the γ_2-types, respectively, while the error bars represent the NSW flows showing the variation of H. The dashed curve shows the value of H, as obtained from the direct numerical simulations of TW solutions of Eqs.(1),(2) [10]. The vertical lines demarcate between the various regions: I- the linearly stable domain; II- the domain where only TW flows of the γ_1-type emerge; III- the domain where TW flows of both γ_1 and γ_2-types coexist; IV- the domain where only TW flows of the γ_2-type emerge; V- the domain where the solutions lose the positivity of Q.

It is important to emphasize that the γ_1-type TW computed here in the range of $R_1 \leq R \leq 7.4$ ($h_1 \leq h_N \leq 2.455$), are very similar in their amplitude and topology to those obtained by Scheid et al. [10] using AUTO software designed for search for TW solutions.

Scheid et al. [10] investigated TW solutions for Eqs.(1), (2) and found that the γ_1-branch bifurcating at $R = R_1$ exists until $R = 9$ (their $Re = 6$) and corresponding to $h_N = 2.621$, extends even further into the domain of higher R, as communicated to us by B.Scheid. We have attempted to follow our γ_1- branch from $R = 7.4$ ($h_N = 2.455$) and on, using both the "standard" initial condition, the continuation method starting from the solutions of the γ_1-type of [10] and also from the solutions of our γ_1-branch at $R \approx 7.4$ ($h_N \approx 2.455$) as initial conditions. However, the ensuing evolution has resulted in the emergence of the corresponding TW solutions on the γ_2- branch. Therefore, our conclusion is that the γ_1- branch becomes unstable for $R > 7.4$ ($h_N > 2.455$).

As follows from our computations, all solutions of Eqs.(1),(2) in case A are TW in the range $2 < R \leq 31$ ($1.587 < h_N \leq 3.958$) and $33 \leq R \leq 35$ ($4.041 \leq h_N \leq 4.121$), with a general trend of increasing the peak-to-peak sizes of both H and Q with increase of R. Along with increase of the peak-to-peak size of Q, there are both increase of Q_{max} and decrease of Q_{min}, so that at

$R \approx 17$ ($h_N \approx 3.240$), the value of Q_{min} approaches zero, and for $R > 17$ ($h_N > 3.240$), Q_{min} becomes negative and remains negative in a certain range $X_1(t;R) < X < X_2(t;R)$ below the depression of the film interface. This range expands with increase of R.

4.1.3. Non-stationary wave solutions As noted above, Eqs.(1),(2) admit along with TW solutions also NSW solutions. In case A the NSW flows are obtained in the range of relatively large Reynolds numbers, $31.5 \leq R \leq 32.5$ ($3.979 \leq h_N \leq 4.021$).

4.1.4. Coexisting solutions As noted above, a domain of coexisting γ_1- and γ_2- TW was found to be $6.7 \leq R \leq 7.6$ ($2.375 \leq h_N \leq 2.477$), see region III in Fig.2. It is important to note that the solutions displayed in Fig.2 were obtained using the "standard" initial condition and the method of continuation from the solutions obtained for adjacent values of R. However, the coexisting γ_2- branch whose emergence is noted above, was obtained in the range $6.7 \leq R \leq 7.6$ ($2.375 \leq h_N \leq 2.477$) solely by initiating the continuation from TW at $R = 7$ ($h_N = 2.410$).

4.2. Case B

4.2.1. Bifurcation structure Figure 3 displays the bifurcation diagram for case B in the plane $\varepsilon - H$. We have divided the investigated domain $0.002 \leq \varepsilon \leq \varepsilon_1$ ($6.840 \times 10^{-3} \leq k \leq k_1$) into several regions where solutions of Eqs.(1),(2) possess different properties. In region I ($\varepsilon \geq \varepsilon_1$) the base Nusselt state $h = h_N,\ q = q_N$ is linearly stable. In region II ($0.0045 \leq \varepsilon < \varepsilon_1$) Eqs.(1),(2) display only TW solutions of the γ_1-type shown by the black squares. This γ_1-branch continues a little further up to the point at $\varepsilon = 0.00425$ ($k = 1.454 \times 10^{-2}$) located in the vicinity of the intersection point (IP) found by Scheid et al. [10], see their Fig.3. The amplitude H of these solutions is in a very good agreement with the results obtained by Scheid et al. [10] for TW solutions. In the narrow region III located in the neighborhood of IP the coexistence between TW flows of both γ_1- and γ_2-families, shown by black triangles, takes place. This coexistence is similar to that obtained in case A and we again conjecture that the emergence of the γ_2-type TW is due to a secondary subcritical pitchfork bifurcation. In region IV the γ_2-type TW flow found within region III at $\varepsilon = 0.00435$ ($k = 1.488 \times 10^{-2}$) is followed by the γ_2-branch indicated by the black triangles, up to $\varepsilon = 0.00374$ ($k = 1.279 \times 10^{-2}$). The emergence of the TW branch of γ_2-type following the domain of coexistence of both types of TW is similar to case A. However, the differences between these two cases are found to the left of region IV. Region V contains interdispersed solutions of the γ_2-type both TW and NSW solutions (shown by error bars with triangles), as well as NSW solutions switching between the γ_1- and the γ_2-types (shown by error bars with $\times$), and also TW flows of the γ_1-family (shown by black squares). The latter represent replication of uni-humped TW solutions of Eqs.(1), (2) located along the ascending branch of TW within region II.

In addition to the waveforms described above, there exists a γ_1-type NSW (shown by error bars with black squares) which appears in the vicinity of the lowest TW at $\varepsilon \approx 0.00425$. This point is within region IV and may be reminiscent of the γ_1-branch of TW going through IP found by Scheid et al.[10]. Thus, we conjecture that the γ_1-branch found by Scheid et al.[10] is unstable. We recall that a similar abrupt termination of the γ_1-branch is found in case A beyond $R = 7.4$ ($h_N = 2.455$) corresponding to their $Re = 4.9$.

4.2.2. Traveling wave solutions Comparing between the solutions obtained here and the TW solutions found in [10] and shown there in Fig.4, both for Eqs.(1),(2), we note that the TW solutions presented in Fig.4a,b,c of Ref.[10] for $k = 0.0256, 0.0169$ and 0.0128, respectively, agree well with the corresponding flows we obtain for $\varepsilon = 0.00748, 0.00494$ and 0.00374, respectively. However, our solution for $\varepsilon = 0.002456$ is found to be an NSW, and not TW, as that displayed

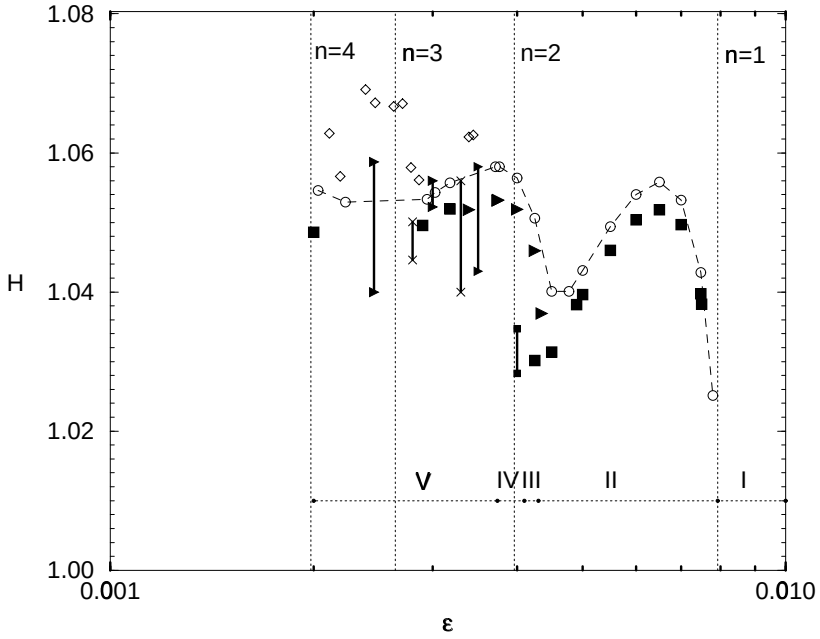

Figure 3. The bifurcation diagram for case B, as obtained from Eqs.(1),(2) that shows the normalized wave amplitude H as a function of ε. The black squares and triangles represent TW flows of γ_1- and γ_2-type, respectively, as obtained from Eqs.(1),(2). The error bars represent the variation of H in the case of the corresponding NSW flows: marked by a black triangle or square when the corresponding NSW is of the γ_2- or γ_1-type, respectively, and marked by $\times$ when it changes its type. The vertical lines $n = 1$ to $n = 4$ represent the linear instability thresholds for the n-th mode, as given by Eq.(18). The black dots indicate the borders between different domains: domain I - the domain of the linear stability of the film; domain II - where only TW solutions for Eqs.(1),(2) of the γ_1-type exist; domain III - the domain of coexistence between TW solutions of both γ_1- and γ_2-types; domain IV - where TW flows of the γ_2-type coexist with NSW solutions; domain V - where TW flows of the γ_2-type emerge along with replicated TW flows of the γ_1-type and NSW of various kinds.

in Fig.4d in [10] obtained for $k = 0.0084$. Thus, while we have not performed a detailed analysis of attraction domains at $\varepsilon = 0.002456$, we conjecture that the γ_2-type TW obtained in [10] there is unstable.

4.2.3. Non-stationary wave solutions The non-stationary solutions found in case B include three types: (i) NSW corresponding to an unstable γ_1-type TW, $\varepsilon = 0.004$ ($k = 1.368 \times 10^{-2}$), indicated in Fig.3 by a bar with black squares; (ii) NSW corresponding to an unstable γ_2-type TW, $\varepsilon = 0.0035, 0.003$ and 0.002456, ($k = 1.197 \times 10^{-2}, 1.026 \times 10{-}2, 0.840 \times 10^{-2}$), all indicated in Fig.3 by bars with black triangles; and (iii) NSW that switches between both the γ_1- and γ_2-waves, $\varepsilon = 0.0033$ ($k = 1.129 \times 10^{-2}$) and 0.0028 ($k = 0.958 \times 10^{-2}$), both indicated in Fig.3 by bars with $\times$. We note that all three types of the NSW flows portray the same power spectrum which contains a noisy variability about the harmonic peaks which is indicative of quasiperiodic tori. Furthermore, we recall that a decrease in ε corresponds to increased nonlinearity. Thus,

the non-stationary phase plane portraits become more dense and their corresponding spectra become more wide banded.

4.2.4. Coexisting solutions As already noted above, Eqs.(1),(2) exhibit coexistence between various types of solutions in case B, as well as in case A. However, unlike case A, where coexistence is found only between two types of TW flows, the coexistence in case B is found also between the γ_2-type TW with an NSW for $\varepsilon = 0.004$ ($k = 1.368 \times 10^{-2}$).

5. Conclusions

In this paper we have carried out a numerical investigation of the nonlinear dynamics of thin falling films in the context of the first-order weighted-residual boundary-layer (WRIBL) equations derived by Ruyer-Quil and Manneville [4]. These equations, augmented with periodic boundary conditions have been shown to admit solutions of various kinds, among which one finds traveling waves (TW) and several types of aperiodic non-stationary waves (NSW). We note that while TW solutions were documented previously by [4, 10], the existence of NSW solutions for Eqs.(1),(2) is first determined in this paper. Furthermore, our numerical investigation of Eqs.(1),(2) shows that the coexistence of stable TW flows is possible in region III for both cases A and B. This result is similar to that of Scheid et al. [10] for the time-independent WRIBL equations (1),(2) in case B. Moreover, additional coexisting forms of TW and NSW are also observed here for the first time in the WRIBL equations with periodic boundary conditions. Based on the results of this investigation of Eqs.(1),(2), we conjecture that several of the solution branches found in the TW analysis[10] are unstable.

The bifurcation structures of the two different cases investigated have several common features: (i) traveling waves of the γ_1-type bifurcate from the stability threshold of the system; (ii) slightly before the parameter range, where the second mode becomes linearly unstable, a coexistence between the traveling waves of γ_1- and γ_2-types arises; (iii) traveling waves of the γ_2-type then become dominant; (iv) the γ_2-type waves then lose stability to a non-stationary flow regime; (v) when more unstable modes become involved in the film dynamics, an increase in complexity of the spatiotemporal film dynamics occurs.

The results of this numerical investigation lead to several open questions that cannot be resolved by this type of analysis: (i) the coexisting γ_1- and γ_2-type TW or the coexisting γ_2-type TW and an NSW, are separated by at least one unstable solution. We conjecture that the former is an outcome of a secondary subcritical pitchfork bifurcation which can explain the steep emergence of the γ_2-type TW branch, at $R \approx 6.7$ ($h_N = 2.375$) in case A and at $\varepsilon \approx 0.004$ ($k = 1.368 \times 10^{-2}$) in case B.

Acknowledgments

This research is partially supported by the Israeli Science Foundation founded by the Israel Academy of Sciences and Humanities and by the Fund for Promotion of Research at the Technion. A. O. was also partially supported by the Technion President Fund and B. and N. Ginsburg Research Fund. We thank Dr. B. Scheid of Université Libre de Bruxelles for fruitful discussions and for sharing with us his unpublished research results.

[1] Oron A, Davis S H and Bankoff S G, 1997, *Rev. Mod. Phys.* **69**, 931.
[2] Benney D J, 1966, *J. Math. Phys.* **45**, 150.
[3] Shkadov V Ya, 1970, *Fluid Dyn.*, **2**, 29.
[4] Ruyer-Quil C and Manneville P, 2000 *Eur. Phys. J. B*, **15**, 357.
[5] Ruyer-Quil C and Manneville P, 2002, *Phys. Fluids*, **14**, 170.
[6] Chang H C, Demekhin E A and Kopelevich D I, 1993, *J. Fluid Mech.*, **250**, 433.
[7] Chang H C, 1994, *Ann. Rev. Fluid Mech.*, **26**, 103.
[8] Benjamin T B, 1957, *J. Fluid Mech.*, **2**, 554.
[9] Yih C S, 1963 *Phys. Fluids*, **6**, 321.

[10] Scheid B, Ruyer-Quil C, Thiele U, Kabov O A, Legros J C and Colinet P, 2005 *J. Fluid Mech.*, **527**, 303.
[11] Oron A and Gottlieb O, 2002, *Phys. Fluids* **14**, 2622.
[12] Gottlieb O and Oron A, 2004 , *Int. J. Bifurcation Chaos*, **14**, 4417.